proceedings

MDPI

Proceedings

Gravitation in the Space with Chimney Topology

Maxim Eingorn [1,*], Andrew McLaughlin II [1], Ezgi Canay [2], Maksym Brilenkov [3] and Alexander Zhuk [4]

[1] Department of Mathematics and Physics, North Carolina Central University, 1801 Fayetteville St., Durham, North Carolina 27707, U.S.A.
[2] Department of Physics, Istanbul Technical University, 34469 Maslak, Istanbul, Turkey
[3] Institute of Theoretical Astrophysics, University of Oslo, P.O. Box 1029 Blindern, N-0315 Oslo, Norway
[4] Astronomical Observatory, Odessa I.I. Mechnikov National University, Dvoryanskaya St. 2, Odessa 65082, Ukraine
* Correspondence: maxim.eingorn@gmail.com

Abstract: Searching for possible indicators of spatial topology of the Universe in the Cosmic Microwave Background data, one recognizes a quite promising interpretation which suggests that the shape of the space manifests itself in the form of anomalies in the large angular scale observations, such as the quadrupole and octopole alignment. Motivated by the presumptive existence of such a tempting connection, we study the chimney topology, $T \times T \times R$, which belongs to the class of toroidal topologies with a preferred direction. The infinite axis in this case may be attributed to the preferred axis of the aforementioned quadrupole and octopole alignment. We investigate the gravitational aspects of such a configuration. Namely, we reveal the form of the gravitational potential, sourced by point-like massive bodies. Starting from the perturbed Einstein equations, which ensure the proper demonstration of relativistic effects, one can derive the Helmholtz equation for the scalar perturbation (gravitational potential). Through distinct alternative methods, we present the physically meaningful nontrivial exact solutions of this equation. Our approach excludes any presumptions regarding the spatial distribution of gravitating sources. We show that the particular solution that appears in the form of summed Yukawa potentials is indeed very convenient for the use in numerical calculations, in the sense that it provides the desired accuracy with fewer terms in the series.

Keywords: spatial topology; gravitational potential; Yukawa interaction

Citation: Lastname, F.; Lastname, F.; Lastname, F. Title. *Proceedings* **2021**, *68*, x. https://doi.org/10.3390/xxxxx

Published: date

1. Introduction

The yet undetermined topology of space, how it may have affected the early evolution of the Universe in the quantum gravity regime and the large scale structure formation at later stages are all vibrant topics of research both in theoretical physics and cosmology. The theory of General Relativity admits any type of spatial topology, so it is quite possible that the Universe is not simply connected, but instead, multiply connected and in the latter case, may have a finite volume with negative or zero curvature [1]. Common examples of multiply connected spaces include spaces with the slab $\boldsymbol{T \times R \times R}$, chimney $\boldsymbol{T \times T \times R}$ and the three torus $\boldsymbol{T \times T \times T}$ topologies, which belong to the class of toroidal topologies in one, two and three dimensions, respectively.

Given the absence of answers on theoretical grounds, there is extensive ongoing research on finding, if any, observational indications of the shape of space [2–6], especially in the Cosmic Microwave Background (CMB) data. Certain compelling studies have pointed out that CMB anomalies in large angular scale observations, namely, the suppression of the quadrupole moment and the quadrupole and octopole alignment, may in fact be consequences of the spatial topology [7,8]. In this connection, we study the chimney

topology with a single infinite axis which may be referred to as the preferred axis of the quadrupole and octopole alignment and the so-called "axis of evil" [9] (see [10] for other potential observable imprints of a preferred axis). From Planck 2013 data [1], the radius of the largest sphere that may be inscribed in the topological domain is bounded from below by $\mathbf{R_i} > \mathbf{0.71}\boldsymbol{\chi}_{\mathrm{rec}}$ for a flat Universe with $\mathbf{T^2 \times R}$ (equal-sided chimney) topology, where $\boldsymbol{\chi}_{\mathrm{rec}}$ ($\sim \mathbf{14}$ Gpc) represents the distance to the recombination surface. There are also former bounds imposed on the size of the Universe by the 7 and 9-year WMAP temperature map data available in [9,11] for the topologies with toroidal dimensions.

In the present work, we consider the space with chimney topology $\boldsymbol{T \times T \times R}$ and study its impacts on the shape of the gravitational potential. In the cosmological context, the potential is sourced by matter density fluctuations [12] and in the Newtonian limit, it is determined in the conventional way by the Poisson equation. Regarding toroidal topologies, the shape of the gravitational potential was previously investigated in [13] and it was shown that a physically meaningful nontrivial solution to the Poisson equation for the $\boldsymbol{T \times T \times R}$ type does not exist. Nevertheless, with the aim to include the relativistic effects in the scheme, one may instead resort to the perturbed Einstein equations, which subsequently yield a Helmholtz-type equation for the gravitational potential [14–16]. Very conveniently, and as we herein demonstrate for the chimney topology, this equation can be solved exactly to give nontrivial and physically meaningful expressions without assuming any particular spatial distribution for the gravitating bodies. Within this latter approach, we elaborate on two alternative solutions for the gravitational potential and demonstrate explicitly that the one in the form of summed Yukawa potentials is the more convenient expression for numerical computation purposes.

2. Methods

Starting with the perturbed Einstein equations to introduce the general relativistic effects into the scheme, one finds that for the concordance ΛCDM cosmological model, the gravitational potential Φ satisfies [14–16]

$$\Delta\Phi_0 - \frac{3\kappa\bar{\rho}c^2}{2a}\Phi_0 = \frac{\kappa c^2}{2a}(\rho - \bar{\rho}), \quad \rho = \sum_n m_n\,\delta(\mathbf{r} - \mathbf{r_n}), \tag{1}$$

where $\kappa \equiv 8\pi G_N/c^4$ (G_N is the Newtonian gravitational constant and c is the speed of light), a denotes the scale factor and Δ is the Laplace operator in comoving coordinates. The comoving mass density and its averaged value are represented by ρ and $\bar{\rho} = \mathrm{const}$, respectively. Delta-shaped gravitating bodies with masses m_n constitute the pressureless matter component of the Universe and imitate, for instance, the galaxies and groups of galaxies. The 0 subscript in Equation (1) indicates that peculiar motion has been omitted in the current setting (see also [17]).

The shifted gravitational potential $\widehat{\Phi}_0 \equiv \Phi_0 - 1/3$ is then straightforwardly determined by

$$\Delta\widehat{\Phi}_0 - \frac{a^2}{\lambda^2}\widehat{\Phi}_0 = \frac{\kappa c^2}{2a}\rho, \quad \lambda \equiv \left(\frac{3\kappa\bar{\rho}c^2}{2a^3}\right)^{-1/2}, \tag{2}$$

which may be solved using the superposition principle.

In the space with chimney topology $T_1 \times T_2 \times R$, we first assign periods l_1 and l_2 to the tori T_1 and T_2 along the x- and y-axes, respectively. In such configuration, there exist infinitely many images for each gravitating source, located at points shifted from its actual position by multiples of l_1 and l_2 along the corresponding axes. Then, for a particle m placed at the center of Cartesian coordinates, the delta functions $\delta(x)$ and $\delta(y)$ read

$$\delta(\mathrm{x}) = \frac{1}{\mathrm{l}_1}\sum_{\mathrm{k}_1=-\infty}^{+\infty}\cos\left(\frac{2\pi\mathrm{k}_1}{\mathrm{l}_1}\mathrm{x}\right), \quad \delta(\mathrm{y}) = \frac{1}{\mathrm{l}_2}\sum_{\mathrm{k}_2=-\infty}^{+\infty}\cos\left(\frac{2\pi\mathrm{k}_2}{\mathrm{l}_2}\mathrm{y}\right), \tag{3}$$

and intrinsically contain the information of the periodic images of the source as well. Given the full form of these functions, the solution to Equation (2) follows as

$$\widehat{\Phi}_0 = -\frac{\kappa c^2}{4a}\frac{m}{l_1 l_2}\sum_{k_1=-\infty}^{+\infty}\sum_{k_2=-\infty}^{+\infty}\left[4\pi^2\left(\frac{k_1^2}{l_1^2}+\frac{k_2^2}{l_2^2}\right)+\frac{a^2}{\lambda^2}\right]^{-1/2}$$
$$\times \exp\left(-\sqrt{4\pi^2\left(\frac{k_1^2}{l_1^2}+\frac{k_2^2}{l_2^2}\right)+\frac{a^2}{\lambda^2}}|z|\right)\cos\left(\frac{2\pi\mathrm{k}_1}{\mathrm{l}_1}\mathrm{x}\right)\cos\left(\frac{2\pi\mathrm{k}_2}{\mathrm{l}_2}\mathrm{y}\right). \tag{4}$$

Now, since Equation (2) is of Helmholtz-type, its solution may also be alternatively obtained by considering the series of Yukawa potentials, each of which corresponds to the individual contribution of the periodic image:

$$\widehat{\Phi}_0 = -\frac{\mathrm{\kappa c}^2 m}{8\pi \mathrm{a}}\sum_{\mathrm{k}_1=-\infty}^{+\infty}\sum_{\mathrm{k}_2=-\infty}^{+\infty}\frac{1}{\sqrt{(x-k_1 l_1)^2+(y-k_2 l_2)^2+z^2}}$$
$$\times \exp\left(-\frac{a\sqrt{(x-k_1 l_1)^2+(y-k_2 l_2)^2+z^2}}{\lambda}\right). \tag{5}$$

As we have indicated earlier, Equations (1) and, therefore, (2) do not incorporate the effects of peculiar motion. In [18], however, it has been shown that the role of such contribution is essential in the cosmological setting and that peculiar velocities may be effectively reintroduced by using the effective cosmological screening length λ_{eff} (see formula (41) of [18]) in replacement of the screening length λ in Equations (1) and (2). At this point, this amounts to substituting λ with λ_{eff} in the right-hand side of (4) and (5), which yields

$$\widetilde{\Phi}_{cos} \equiv \left(-\frac{\kappa c^2}{8\pi a}\frac{m}{l}\right)^{-1}\widehat{\Phi}_{cos} = \sum_{k_1=-\infty}^{+\infty}\sum_{k_2=-\infty}^{+\infty}\left(k_1^2+k_2^2+\frac{1}{4\pi^2\tilde{\lambda}_{eff}^2}\right)^{-1/2}$$
$$\times \exp\left(-\sqrt{4\pi^2(k_1^2+k_2^2)+\frac{1}{\tilde{\lambda}_{eff}^2}}|\tilde{z}|\right)cos(2\pi k_1\tilde{x})\,cos(2\pi k_2\tilde{y}) \tag{6}$$

and

$$\widetilde{\Phi}_{exp} \equiv \left(-\frac{\kappa c^2}{8\pi a}\frac{m}{l}\right)^{-1}\widehat{\Phi}_{exp} = \sum_{k_1=-\infty}^{+\infty}\sum_{k_2=-\infty}^{+\infty}\frac{1}{\sqrt{(\tilde{x}-k_1)^2+(\tilde{y}-k_2)^2+\tilde{z}^2}}$$
$$\times \exp\left(-\frac{\sqrt{(\tilde{x}-k_1)^2+(\tilde{y}-k_2)^2+\tilde{z}^2}}{\tilde{\lambda}_{\mathrm{eff}}}\right), \tag{7}$$

where we have also employed the rescaled quantities $\mathrm{x} = \tilde{\mathrm{x}}\mathrm{l}, \mathrm{y} = \tilde{\mathrm{y}}\mathrm{l}, \mathrm{z} = \tilde{\mathrm{z}}\mathrm{l}, \lambda_{\mathrm{eff}} = \tilde{\lambda}_{\mathrm{eff}}a\mathrm{l}$ and for simpler representation, set $\mathrm{l}_1 = \mathrm{l}_2 = \mathrm{l}$. The labels cos and exp have been introduced in the above set to distinguish between two forms of the solution. Since peculiar velocities are effectively restored, the 0 subscripts have been eliminated.

Both formulas (6) and (7) specify the gravitational potential attributed to a point-like body with mass m, located at the point $(x, y, z) = (0,0,0)$ in Cartesian coordinates, together with its images at points $(x, y, z) = (k_1 l, k_2 l, 0)$ for $k_{1,2} = 0, \pm 1, \pm 2, \ldots$ Evidently, since these rescaled potentials consist of infinite series, it is necessary to know the minimum number of terms required to calculate them numerically for any order of accuracy. As to the accuracy adopted in our work, we demand that this number n is determined in such a way to keep the absolute value of the ratio (exact $\tilde{\Phi}$ - approximate $\tilde{\Phi}$) / (exact $\tilde{\Phi}$) less than 0.001. It may, of course, differ for the alternative formulas, so we label these numbers as n_{exp} and $n_{\cos}$, correspondingly. The formula which admits the smaller n serves as a better tool for numerical analysis.

In the following section, we present our results regarding the comparison of the formulas (6) and (7) based on the above mentioned criterion. Since these expressions contain double series, we use Mathematica [19] for generating the sequence of pairs (k_1, k_2) in the increasing order of $\sqrt{k_1^2 + k_2^2}$. Then, n is ascribed the number of combinations providing the desired precision.

3. Results

For demonstration purposes, we have chosen eight points on the rescaled coordinates and used Mathematica [19] to calculate the exact value of the gravitational potential at these points by the formula (7) for $n \gg n_{\text{exp}}$. The results are shown in Table 1 for two cases $\tilde{\lambda}_{\text{eff}} = 0.01$ and $\tilde{\lambda}_{\text{eff}} = 0.1$. Provided that $n \geq n_{\text{exp}}$, the approximate value of $\tilde{\Phi}_{\text{exp}}$ (from (7)) agrees with the exact one up to one tenth of a percent. The minimum numbers of terms needed in the alternative formula (6) to obtain these potential values, again, up to one tenth of a percent, correspond to the $n_{\cos}$ columns.

Table 1. The rescaled gravitational potential $\tilde{\Phi}$ and numbers n_{exp} and $n_{\cos}$ of terms in series at eight selected points for $\tilde{\lambda}_{\text{eff}} = 0.01$ and $\tilde{\lambda}_{\text{eff}} = 0.1$ in the left and right charts, respectively. The dash hides incorrect outputs produced due to computational complications.

	$\tilde{x}$	$\tilde{y}$	$\tilde{z}$	$\tilde{\Phi}$	n_{exp}	$n_{\cos}$
A_1	0.5	0	0.5	5.524×10^{-31}	2	1007
A_2	0.5	0	0.1	2.810×10^{-22}	2	—
A_3	0.5	0	0	7.715×10^{-22}	2	—
B_1	0.1	0	0.5	1.405×10^{-22}	1	187
B_2	0.1	0	0.1	5.101×10^{-6}	1	2119
B_3	0.1	0	0	4.540×10^{-4}	1	—
C_1	0	0	0.5	3.857×10^{-22}	1	236
C_2	0	0	0.1	4.540×10^{-4}	1	1479

	$\tilde{x}$	$\tilde{y}$	$\tilde{z}$	$\tilde{\Phi}$	n_{exp}	$n_{\cos}$
A_1	0.5	0	0.5	2.418×10^{-3}	7	40
A_2	0.5	0	0.1	2.398×10^{-2}	6	808
A_3	0.5	0	0	2.700×10^{-2}	4	—
B_1	0.1	0	0.5	1.203×10^{-2}	4	28
B_2	0.1	0	0.1	1.719	1	380
B_3	0.1	0	0	3.679	1	—
C_1	0	0	0.5	1.353×10^{-2}	4	37
C_2	0	0	0.1	3.679	1	490

The data in Table 1 clearly illustrate that the formula (7) is a better option than its alternative for reducing the computational cost in numerical analysis as $n_{\text{exp}} \ll n_{\cos}$. It is worth noting that the selected values of $\tilde{\lambda}_{\text{eff}}$ serve well in depicting the observable Universe as they both satisfy $\tilde{\lambda}_{\text{eff}} < 1$: for the chimney topology studied here, the lower bound on physical periods al of the tori is of the order of 20 Gpc [1]. Additionally, according to [18], the current value of the effective screening length is approximately 2.6 Gpc, so the ratio $\lambda_{\text{eff}}/(al)$, in terms of these values, limits the physically interesting range for $\tilde{\lambda}_{\text{eff}}$ today.

Finally, we present Figure 1 to help visualize the shape of the rescaled gravitational potential $\tilde{\Phi}$ for two different values of $\tilde{\lambda}_{\text{eff}}$ considered in Table 1. To plot these figures, we have used Mathematica [19] and employed the formula (7) for $n \gg n_{\text{exp}}$.

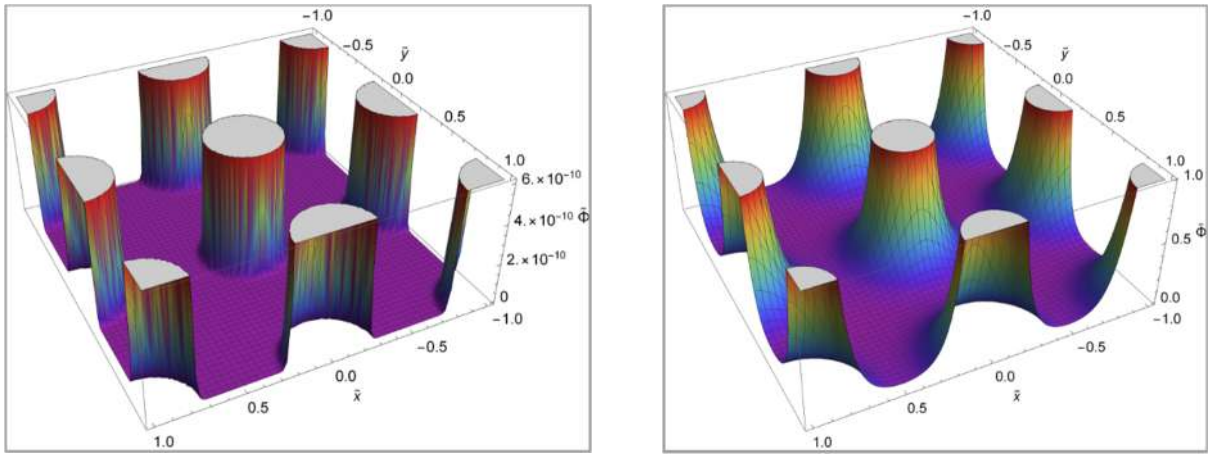

(**a**) (**b**)

Figure 1. Rescaled gravitational potential $\tilde{\Phi}$ for $z = 0$ (**a**) for $\tilde{\lambda}_{\text{eff}} = 0.01$; (**b**) for $\tilde{\lambda}_{\text{eff}} = 0.1$.

4. Conclusions

In the present work we have elaborated on two alternative methods to reveal the form of the gravitational potential for the chimney topology $T \times T \times R$ of the Universe. One of the solutions (see Equation (6)) has been obtained by Fourier expanding the delta functions using periodicity along two toroidal dimensions in the model. The other one (see Equation (7)) has been presented as the plain summation of the solutions to the Helmholtz equation, for the source particle and its images, all of which admit Yukawa-type potential expressions. Meanwhile, we have emphasized the essential role of the effective screening length $\tilde{\lambda}_{\text{eff}}$, which specifies the cutoff distance of the gravitational interaction in the cosmological setting, manifested explicitly in this latter expression.

Having obtained two alternative formulas for the gravitational potential, we then demonstrated that the solution containing the series sum of Yukawa potentials is a better choice for use in numerical calculations, in the sense that the desired accuracy is attained by keeping fewer terms in the series in the physically significant cases when $\tilde{\lambda}_{\text{eff}} < 1$.

Acknowledgments: The work of M. Eingorn and A. McLaughlin II was supported by National Science Foundation (HRD Award #1954454).

Author Contributions: M.E.: Conceptualization, Methodology, Formal analysis, Investigation, Writing – Review & Editing, Visualization, Supervision, Project administration, Funding acquisition. A.M.II: Formal analysis, Investigation, Visualization. E.C.: Formal analysis, Investigation, Writing – Original Draft. M.B.: Formal analysis, Investigation. A.Z.: Methodology, Formal analysis, Investigation, Supervision.

Conflicts of Interest: The authors declare no conflict of interest. The funding sponsors had no role in the design of the study; in the collection, analyses, or interpretation of data; in the writing of the manuscript, and in the decision to publish the results.

References

1. Ade P.A.R. et al. [Planck Collaboration]. Planck 2013 results. XXVI. Background geometry and topology of the Universe. *A&A* **2014**, *571*, A26, DOI: 10.1051/0004-6361/201321546. arXiv:1303.5086 [astro-ph.CO].
2. Bielewicz P.; Riazuelo A. The study of topology of the universe using multipole vectors. *Mon. Not. R. Astron. Soc.* **2009**, *396*, 609, DOI: 10.1111/j.1365-2966.2009.14682.x. arXiv:0804.2437 [astro-ph].
3. Bielewicz P.; Banday A.J. and Gorski K.M. Constraining the topology of the Universe using the polarized CMB maps. *Mon. Not. R. Astron. Soc.* **2012,** *421*, 1064, DOI: 10.1111/j.1365-2966.2011.20371.x. arXiv: 1111.6046 [astro-ph.CO].
4. Vaudrevange P.M.; Starkman G.D.; Cornish N.J. and Spergel D.N. Constraints on the topology of the Universe: Extension to general geometries. *Phys. Rev. D* **2012,** *86*, 083526, DOI: 10.1103/PhysRevD.86.083526. arXiv:1206.2939 [astro-ph.CO].

5. Fabre O.; Prunet S. and Uzan J.-P. Topology beyond the horizon: how far can it be probed? *Phys. Rev. D* **2015,** *92,* 043003, DOI: 10.1103/PhysRevD.92.043003. arXiv:1311.3509 [astro-ph.CO].
6. Ade P.A.R. et al. [Planck Collaboration]. Planck 2015 results. XVIII. Background geometry and topology. *A&A* **2016**, *594,* A18, DOI: 10.1051/0004-6361/201525829. arXiv:1502.01593 [astro-ph.CO].
7. Bielewicz P.; Banday A.J. Constraints on the topology of the Universe derived from the 7-year WMAP data. *Mon. Not. R. Astron. Soc.* **2011,** *412*, 2104, DOI: 10.1111/j.1365-2966.2010.18057.x. arXiv:1012.3549 [astro-ph.CO].
8. Bielewicz P.; Banday A.J. and Gorski K.M. Constraints on the topology of the Universe derived from the 7-year WMAP CMB data and prospects of constraining the topology using CMB polarization maps. Proceedings of the XLVIIth Rencontres de Moriond, La Thuile, Italy, March 2012; Eds. Auge E.; Dumarchez J. and Tran Thanh Van J.; ARISF; p. 91. arXiv:1303.4004 [astro-ph.CO].
9. Aslanyan G.; Manohar A.V. The topology and size of the Universe from the Cosmic Microwave Background. *JCAP* **2012,** *06*, 003, DOI: 10.1088/1475-7516/2012/06/003. arXiv:1104.0015 [astro-ph.CO].
10. Floratos E.G.; Leontaris G.K. On topological modifications of Newton's law. *JCAP* **2012,** *04*, 024, DOI: 10.1088/1475-7516/2012/04/024. arXiv:1202.6067 [astro-ph.CO].
11. Aslanyan G.; Manohar A.V. and Yadav A.P.S. The topology and size of the Universe from CMB temperature and polarization data. *JCAP* **2013**, *08*, 009, DOI: 10.1088/1475-7516/2013/08/009. arXiv:1304.1811 [astro-ph.CO].
12. Peebles P.J.E. *The large-scale structure of the Universe*; Princeton University Press: Princeton, 1980.
13. Brilenkov M.; Eingorn M. and Zhuk A. Lattice Universe: examples and problems. *EPJC* **2015**, *75*, 217, DOI: 10.1140/epjc/s10052-015-3445-2. arXiv:1410.3909 [gr-qc].
14. Eingorn M. First-order cosmological perturbations engendered by point-like masses. *Astrophys. J.* **2016**, *825*, 84, DOI: 10.3847/0004-637X/825/2/84. arXiv:1509.03835 [gr-qc].
15. Eingorn M.; Kiefer C. and Zhuk A. Scalar and vector perturbations in a universe with discrete and continuous matter sources. *JCAP* **2016**, *09*, 032, DOI: 10.1088/1475-7516/2016/09/032. arXiv:1607.03394 [gr-qc].
16. Eingorn M.; Kiefer C. and Zhuk A. Cosmic screening of the gravitational interaction. *Int. J. Mod. Phys. D* **2017,** *26*, 1743012, DOI: 10.1142/S021827181743012X. arXiv:1711.01759[gr-qc].
17. Eingorn M. Cosmological law of universal gravitation. *Int. J. Mod. Phys. D* **2017**, *26*, 1750121, DOI: 10.1142/S0218271817501218. arXiv:1709.02264 [gr-qc].
18. Canay E.; Eingorn M. Duel of cosmological screening lengths. *Phys. Dark Univ.* **2020,** *29*, 100565, DOI: 10.1016/j.dark.2020.100565. arXiv:2002.00437 [gr-qc].
19. Wolfram Research, Inc., Mathematica, Version 11.3, Champaign, IL, 2018.